SOUTHERN CALIFORNIA EARTHQUAKE CENTER

Title of Project: Research toward the Master Model/
Northern California Seismicity Simulations
Name of PI: Steven N. Ward
Institution: University of California, Santa Cruz

Annual Report, 1999

Seismicity Simulations:

Much of my SCEC funded research in 1999 dealt with computer simulations of seismicity on the fault system of Northern California. The work was done in conjunction with the USGS working group WGNCEP/99 that just released a new round of earthquake probabilities for the San Francisco Bay region in October, 1999. The paper that describes my earthquake simulations [**Ward, S. N., 2000. San Francisco Bay Area Earthquake Simulations: A step toward a Standard Physical Earthquake Model**] was revised 1999 and worked its way though the review process. The paper will appear in the April 2000 issue of BSSA. In 2000, I will apply the technique to the fault system of southern California.

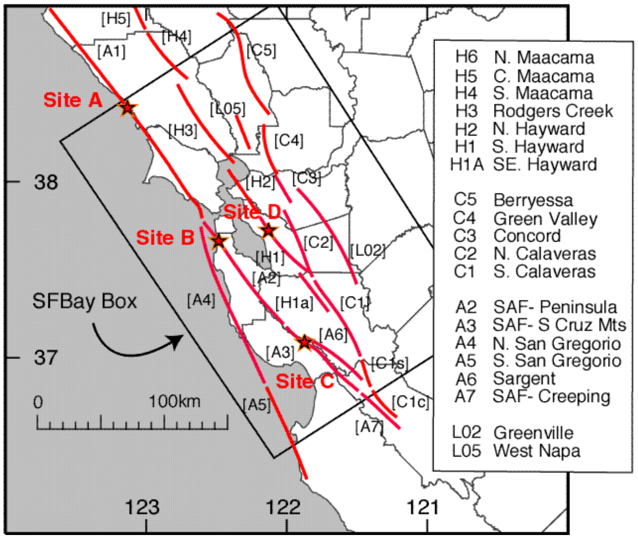

Figure 1. Map of Bay Area faults included in the Northern California seismicity simulations. Sites A to D are locations where site specific probabilities are calculated.

Summary: Earthquakes in California's San Francisco Bay Area are likely to be more strongly affected by elastic stress interaction than earthquakes in any other place in the world because of the region's closely spaced, sub-parallel distribution of faults (Figure 1). As such, I believe that meaningful quantification of earthquake probability and hazard in the Bay Area can be made only with the guidance provided by physically-based and region-wide earthquake models that account for this interaction. This effort represents a first step in developing a *Standard Physical Earthquake Model* for the San Francisco Bay Area through realistic, 3000-year simulations of earthquakes on all of the area's major faults (Figures 2 and 3). These simulations demonstrate that a *Standard Physical Earthquake Model* is entirely feasible, they illustrate its application, and they blueprint its construction. A *Standard Physical Earthquake Model* provides the mechanism to integrate fully the diverse disciplines within the earthquake research community. As a platform for data utilization and verification, a physical earthquake model can employ directly any earthquake property

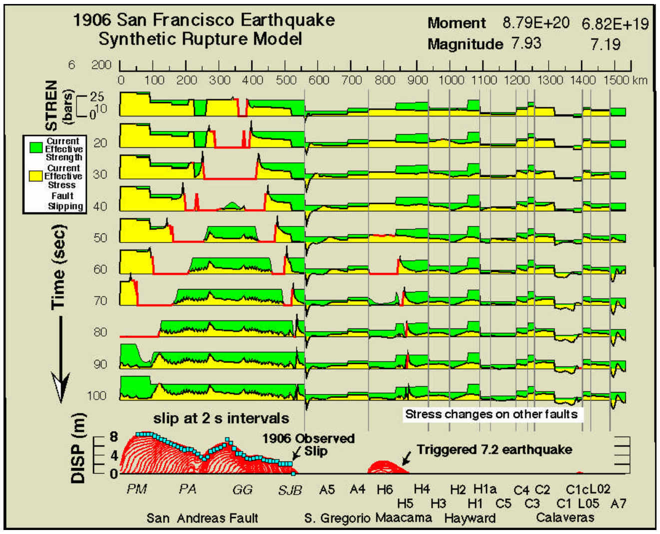

Figure 2. Calculated stress effects of the 1906 San Francisco earthquake. To the left appears the developing 1906 rupture. To the right are the time-dependent induced changes in effective stress on all of the other faults of the system. Vertical lines separate individual faults. During rupture, Coulomb stresses can rise then fall, or vice-versa. Intra-rupture stresses may not resemble the final static condition. In this case, a M7.2 earthquake on the North Maacama Fault was triggered some 50 seconds after nucleation of the main event.

that is measurable in the field or in the laboratory to tune and test its seismicity products. As a platform for probability forecasts, a physical earthquake model can supply rational estimates of every imaginable earthquake statistic while simultaneously satisfying all slip and earthquake rate constraints (Figures 4 and 5). As a platform for hazard analysis, a physical earthquake model can compute earthquake-shaking intensity from first principles by convolving a full suite of rupture scenarios with site-specific dislocation Green’s functions.

Physical earthquake models have advanced greatly in the last decade. Simulations of earthquake generation and recurrence are now sufficiently credible that such calculations must begin to take substantial roles in scientific studies of earthquake probability and hazard.

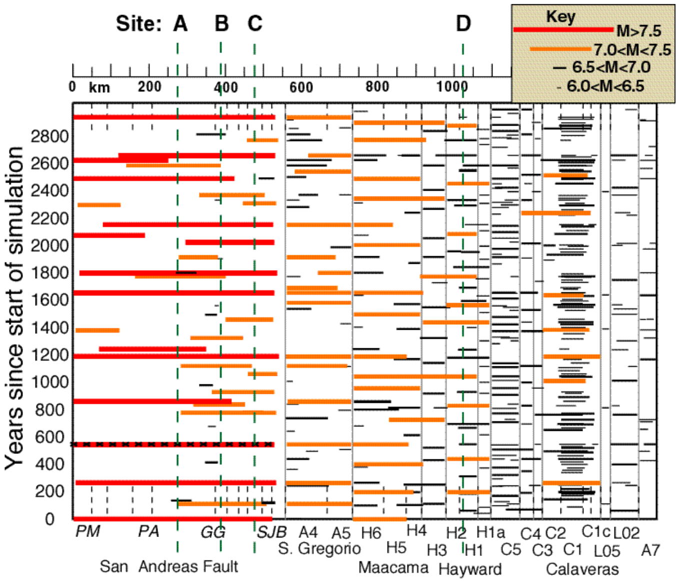

Figure 4. 3000-year space-time sequence of earthquakes over the full northern California fault system. Fault segment codes are the same as in Figure 1. Statistics of earthquake recurrence extracted from events that ruptured through the four sites A-D (vertical dashed lines) and the date of the last event form the basis for the probability forecasts in Figure 5

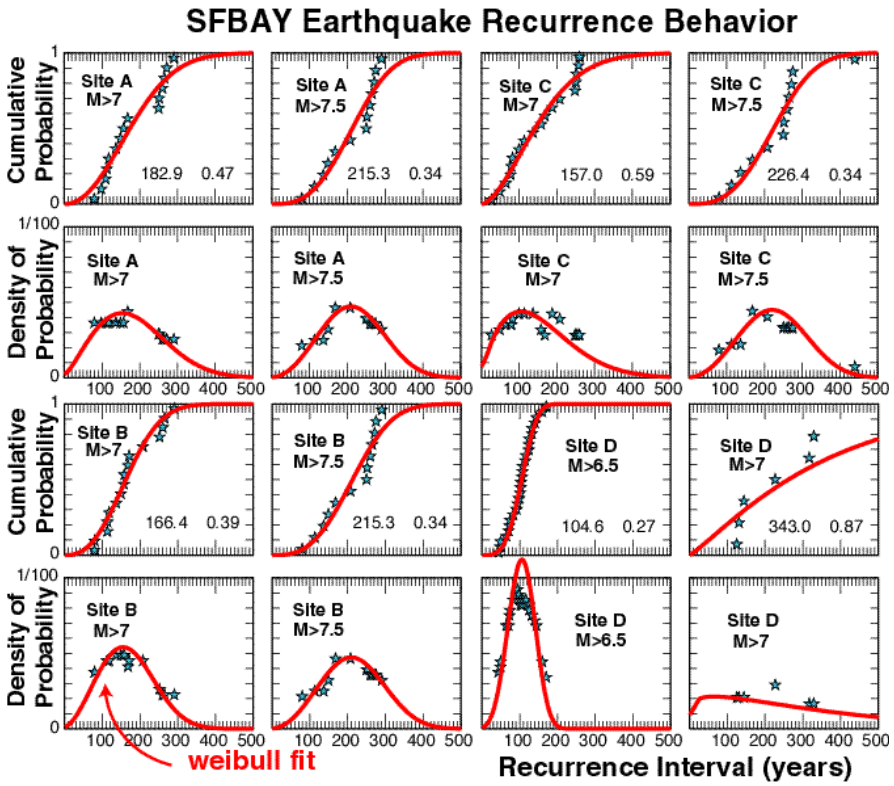

Figure 5. The stars show the earthquake recurrence distribution for M>7 and M>7.5 events at sites A, B and C; and for M>6.5 and M>7 events at site D (no event >7.5 happened on the Hayward) as derived from the simulation. Both cumulative probability and probability density are plotted. Earthquake probabilities could be extracted directly from the “stars” in the Figure, however it is traditional to fit the data with a smooth curve that has a small number of parameters, and then compute probabilities from the curve. The red curves in this Figure are Weibull function fits to the data. Weibull functions have two parameters: a mean value (T_{ave}) in years and an aperiodicity coefficient (AC). Both of these numbers are listed in the panels for each site. AC=0 means perfect regularity. AC=1 is Poisson. 0<AC<1 means quasi-periodic. AC>1 means clustered.

Consistency of Earthquake Moment Rates, and Space Geodetic Strain.

In 1999, I continued to consider the issue of the consistency of earthquake moment rates, geological fault data, and space geodetic strain. In particular, new and dense GPS data have become available such that, when combined with SCEC Velmap2, geodetic strain rates can be estimated everywhere in California, if not the entire North American continent. Figures 6 and 7 show my most recent mappings of the geodetic strain rates over California/Nevada and all of the United States.

Admittedly, outside of California, GPS data is still sparse and many of the features of Figure 7 may not be statistically robust or directly related to tectonics. Nevertheless, I suggest that mapping of geodetic strain rate over continental wide regions is the wave of the future.

Compared with past results [Ward, 1998], I find that geodetic moment rates for southern and northern California are about 10 and 40% higher respectively.

In the upcoming year, I will use maps like Figure 6 to produce a purely GPS-based earthquake source characterization for SCEC's Working-Group 2000.

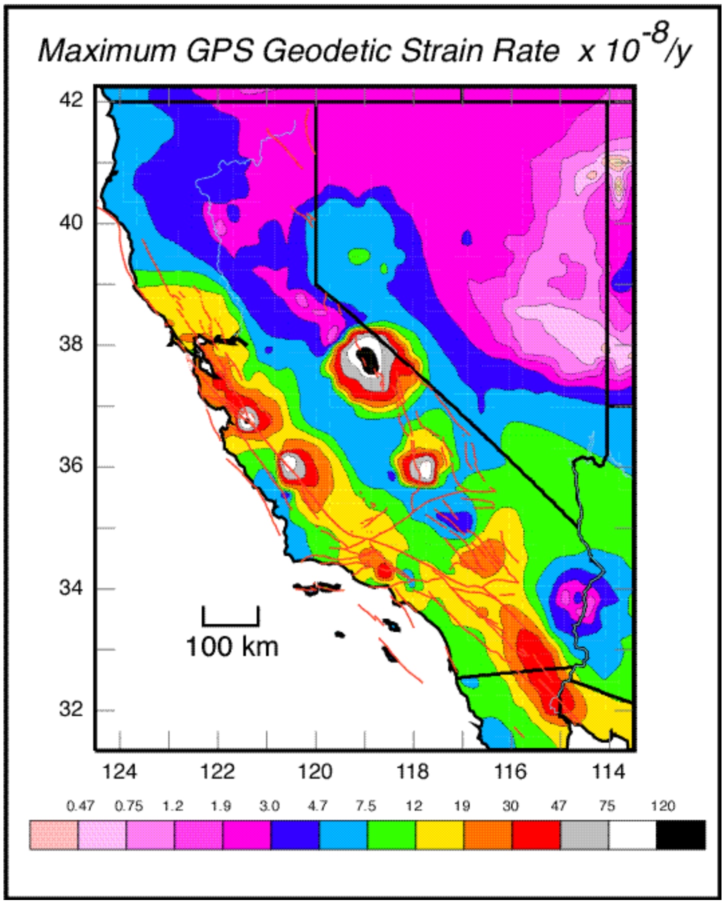

Figure 6. Maximum geodetic strain rates in units of 10^{-8}/y as determined from space geodetic data. Peak strains often are found in volcanic fields like Mammoth Lakes and Coso.

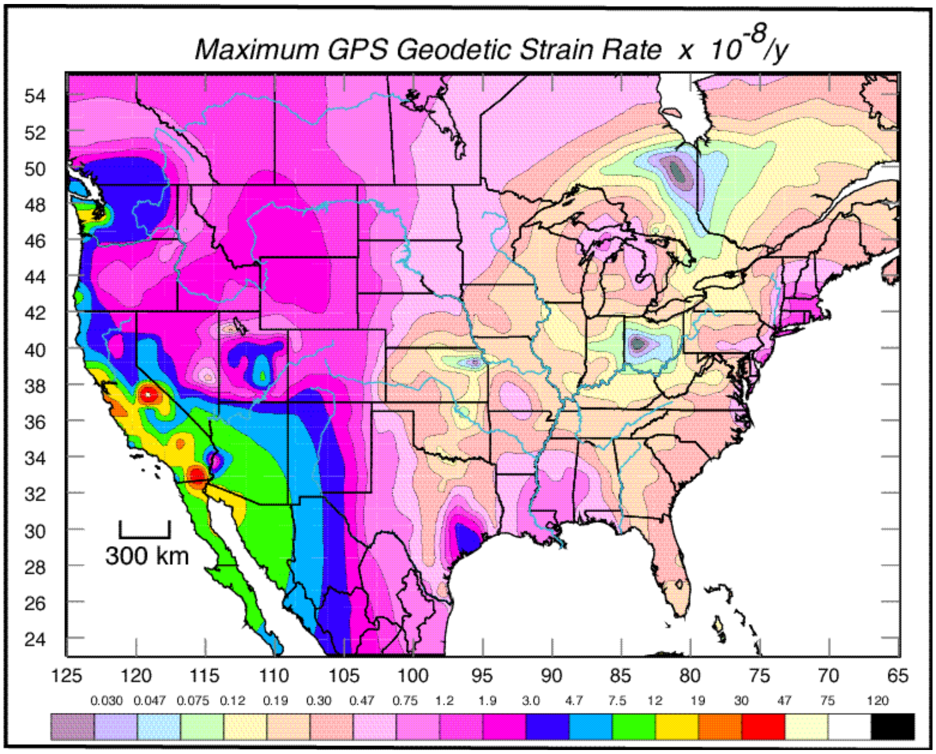

Figure 7. Maximum geodetic strain rates in units of 10^{-8}/y as determined from space geodetic data. Strain rates in the United States vary by over a factor of 1000 from <0.03 x10^{-8}/y in the Central/Southeast to >30x10^{-8}/y in southern California.

Probabilistic hazard of tsunami from earthquakes and submarine landslides in the southern California borderland.

1999 saw progress in developing methods of probabilistic analysis to tsunami hazard. Probabilistic hazard calculations for earthquake and landslide-generated submarine tsunami parallel those that I recently developed for asteroid impact [Ward and Asphaug, 2000]. Hazard analysis keys on u_z^{crit}, a specified tsunami amplitude for which the probability of exceedence is desired. The primary elements in the calculation are:

1) Frequency of occurrence of landslides/earthquakes of given features (length, width, thickness, slide velocity, moment, etc.) at every offshore location $\mathbf{r}_o$.

2) Mean maximum tsunami height $A_{max}(\mathbf{r}_o)$ atop the source that are generated by landslides/earthquakes of given features in water of depth h_0.

3) Tsunami amplitude loss in propagating from the source location $\mathbf{r}_o$ to coast location $\mathbf{r}_s$. Amplitude loss includes both the effects of geometrical spreading and frequency dispersion.

4) Tsunami amplitude gain due to shoaling on approach to $\mathbf{r}_s$.

5) Statistical uncertainties on each of 1 to 4.

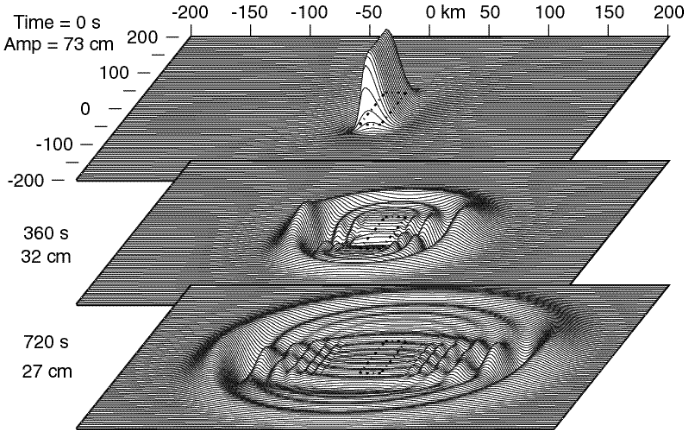

Figure 8. Views of the expanding tsunami rings from a M7.5 thrust earthquake. Elapsed time in seconds and maximum amplitude in cm are given at the left and right sides. The dashed rectangle in the center traces the surface projection of the 45^0 dipping fault. For large earthquakes, nearly all tsunami energy beams perpendicular to the strike of the fault (*toward the left and right in this picture*).

Given (1) to (5), the total rate $N_{exceed}(u_z^{crit}, \mathbf{r}_s)$ of tsunami exceeding u_z^{crit} at each $\mathbf{r}_s$ is obtained in the same way as is done in seismic analysis -- by integrating the rates of all admissible tsunami sources and tsunami locations $\mathbf{r}_o$. Admissible means only those earthquakes/slides at $\mathbf{r}_o$ that are capable of generating tsunami larger than u_z^{crit} at $\mathbf{r}_s$.

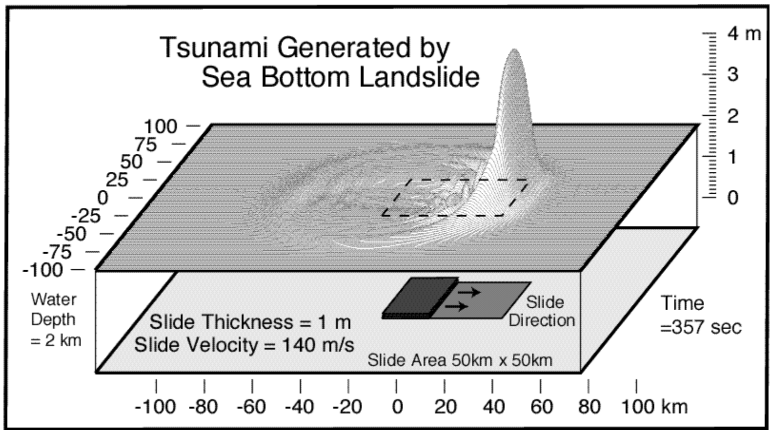

Figure 9. Tsunami produced by a submarine landslide. The slide is 1-m thick and occurs over a 50km by 50km area. The slide starts to the left and moves to the right at 140 m/s. Note the strong amplification of the wave in the slide direction.

In dealing with statistical hazards that include considerable uncertainties, elements 1 to 4 can be generalized. For instance, modeling (Figures 8 and 9) may conclude that earthquake moment M and landslide volume V are the principal drivers of tsunami amplitude. In this case, 1) may be served by a power laws such as $N_>(V)=10^{a-bV}$ or $N_>(M)=10^{a-bM}$. For landslides, the b-value may be a universal scaling parameter as it is for earthquakes. The a-value represents the total slide activity of a region – this likely depends on the stratigraphic coherence of the shallow seabed, mean slope, sediment rate, etc. Probabilistic tsunami hazard analysis is young, but it should produce a product within a year. I think that this work is a wonderful example of the knowledge transfer that SCEC has fostered.

SCEC Publications in 1999:

Sieh, K., S. N. Ward, D. Natawidjaja and B. W. Suwargadi, 1999. Crustal Deformation at the Sumatran Subduction Zone Revealed by Coral Rings, *Geophys. Res. Lett., 26*, 3141-3144.

Ward, S. N., 2000. San Francisco Bay Area Earthquake Simulations: A step toward a Standard Physical Earthquake Model, *Bull. Seism. Soc. Am.*, in press.

Ward, S. N. and E. Asphaug, 2000. Asteroid Impact Tsunami: A probabilistic hazard assessment, *Icarus*, in press.

Ward, S. N., 2000. “Tsunamis” in *The Encyclopedia of Physical Science and Technology,* ed. R. A. Meyers, Academic Press, in press.